Photo- and electroproduction of $K^0\Lambda$ near threshold and effects of the K^0 electromagnetic form factor

T. Mart

Departemen Fisika, FMIPA, Universitas Indonesia, Depok 16424, Indonesia

(Received 29 September 2010; revised manuscript received 29 March 2011; published 25 April 2011)

By extending our previous isobar model to the $K^0\Lambda$ isospin channel, we investigate the properties of the $K^0\Lambda$ photo- and electroproduction at energies near threshold. It is found that the pseudovector coupling yields significantly larger cross sections. Variation of the K_1 coupling constants has significant effect only on the pseudovector model. The electromagnetic form factor of the neutral kaon K^0 is found to have a sizable effect on the longitudinal cross section of the $K^0\Lambda$ electroproduction near the threshold.

DOI: 10.1103/PhysRevC.83.048203 PACS number(s): 13.60.Le, 13.40.Gp, 14.20.Gk, 25.20.Lj

Recently there has been great interest in the electromagnetic production of the neutral kaon [1,2]. There are several motivations behind this interest, one of them being the search for missing resonances. In the K^0 photoproduction the t-channel K^0 intermediate state does not present due to the lack of interaction between real photons and neutral mesons. The absence of this channel might have a strong impact on the angular distribution of the predicted observables and also increase the dominance of the nucleon resonance contribution. This situation is obviously different in the leading $K^+\Lambda$ [3,4] and $K^+\Sigma^0$ [5] channels, which for years have become the main source of information on the strangeness production process. Another motivation comes from the deuteron sector, in which the relevant processes are $\gamma + d \rightarrow K^0 + \Lambda + p$ and $\gamma + d \rightarrow K^0 + \Sigma^0 + p$. Due to the lack of the neutron target, the two processes are expected to be the natural avenue in the investigation of kaon photoproduction on the neutron. A recent report shows that the extraction of the elementary cross section is possible for these processes in the quasifree scattering region, where the final state interaction effects are negligible [1]. Note that the result of such an analysis relies on the results of the Kaon-Maid model [6], especially on the $K^0\Lambda$ channel. However, the predicted total cross section of this channel is found to be twice larger than that of the $K^+\Lambda$ channel, in contrast to the case of the other four related isospin channels (see Fig. 1 of Ref. [1]).

There was an attempt to investigate the effect of the K^0 charge form factor on the $K^0\Lambda$ electroproduction [7]. Although significant effects on the longitudinal cross section were observed, the result was found to be very model dependent. Consequently, a reliable phenomenological model becomes the important prescription for this purpose. Since a reliable model should not depend on too many uncertain free parameters, it is obviously important to limit the energy of interest very close to the production threshold.

Very recently, we have analyzed photo- and electroproduction of the $K^+\Lambda$ final state at energies near its production threshold by utilizing an isobar model [8]. Using the pseudoscalar (PS) coupling the model can nicely describe experimental data both in the real and virtual photon sectors up to total c.m. energy $W = 50$ MeV above the threshold. By using pseudovector (PV) coupling, agreement with the experimental data can still be achieved, although the χ^2 per number of data points increases from 0.92 to 1.53.

This paper reports on the extension of our previous model to the $K^0\Lambda$ isospin channel. For this purpose we employ the SU(3) symmetry to relate the hadronic coupling constants of the background terms in the two channels, i.e.,

$$g_{K^+\Lambda p} = g_{K^0\Lambda n}, \quad g_{K^+\Sigma^0 p} = -g_{K^0\Sigma^0 n}, \quad g^{V,T}_{K^{*+}\Lambda p} = g^{V,T}_{K^{*0}\Lambda n}. \tag{1}$$

In the $K^0\Lambda$ production, the vector meson exchanged in the t channel is the $K^{*0}(896.10)$. Therefore, the transition moment in K^+ production, $g_{K^{+*}K^+\gamma}$, must be replaced by the neutral transition moment by using [5]

$$g_{K^{*0}K^0\gamma}/g_{K^{*+}K^+\gamma} = -1.53 \pm 0.20. \tag{2}$$

In the case of the $K_1(1270)$ vector meson exchange, there is no sufficient information from the *Particle Data Book* [9]. Thus, we use the value given by the Kaon-Maid [6],

$$r_{K_1K\gamma} \equiv g_{K_1^0K^0\gamma}/g_{K_1^+K^+\gamma} = -0.45, \tag{3}$$

which was extracted from simultaneous fitting of the $K^+\Sigma^0$ and $K^0\Sigma^+$ photoproduction data. The $S_{01}(1800)$ u channel stays unmodified, since from Eq. (1) we have $g_{K^+\Lambda p} = g_{K^0\Lambda n}$, whereas the electromagnetic vertex $\gamma Y^{*0}\Lambda$ in both $K^+\Lambda$ and $K^0\Lambda$ channels is the same.

In the resonance term we have to replace the helicity photon couplings of the proton $A^p_{1/2}$ with that of the neutron, where [9]

$$A^n_{1/2} = -0.015 \pm 0.021 \ \text{GeV}^{-1/2}. \tag{4}$$

Note that this coupling is substantially smaller than the proton coupling, i.e., $A^p_{1/2} = 0.053 \pm 0.016$ GeV$^{-1/2}$ [9]. As a consequence, we may expect a relatively smaller resonance contribution in the case of $K^0\Lambda$ production. This is proven by Fig. 1, where we compare the background and resonance contributions to the total cross section of the $K^+\Lambda$ and $K^0\Lambda$ photoproduction. Different from the $K^+\Lambda$ channel, in which contribution of the $S_{11}(1650)$ resonance is more or less 20%, contribution of this resonance to the $K^0\Lambda$ total cross section at $W = 50$ MeV above threshold is only about 3%.

The predicted $K^0\Lambda$ total cross sections of both PS and PV models are shown in Fig. 2, where the effects of the variation

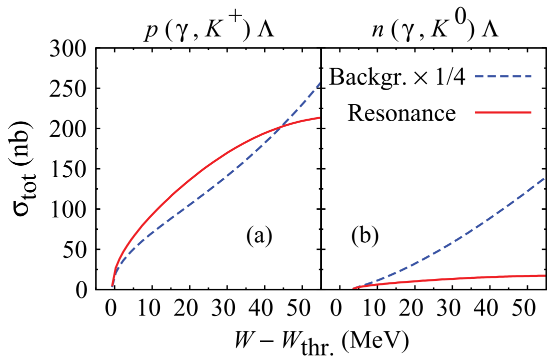

FIG. 1. (Color online) Contributions of the background terms and the $S_{11}(1650)$ resonance to the total cross section of the $\gamma + p \to K^+ + \Lambda$ (a) and $\gamma + n \to K^0 + \Lambda$ (b) channels.

of the ratio $r_{K_1K\gamma}$ given in Eq. (3) are displayed. For the sake of visibility, we have varied this ratio by ±100% (±20%) in the PS (PV) model. Both the cross section and the effect are obviously larger in the PV model. We have found that this phenomenon originates from the large K_1 and K^* couplings in the PV model, especially in the case of K_1, where the coupling constants are around 10 times larger than those in the PS model. Although we believe that the PS model is still better than the PV one, as in the $K^+\Lambda$ case, an experimental check of the $K^0\Lambda$ total cross section is still mandatory to help to clarify this situation.

The difference between the PS and PV models also appears in the differential cross section as shown in Fig. 3. From this figure it is apparent that the dominant role of the K_1 and K^* exchanges in the PV model yields not only a large cross section, but also amplifies the bump structure in the angular distribution of the differential cross section. Therefore, experimental data of the $K^0\Lambda$ differential cross section can shed more light on the role of the K_1 and K^* in kaon photoproduction. From Fig. 3 we can see that both models do not indicate a backward-peaking cross section. This is different from the cross section estimated by the deuteron target [2]. However, we realize that in order to estimate this cross section the ratio $r_{K_1K\gamma}$ is varied [2]. It is important to note here that this ratio is no longer a free parameter if one starts with the elementary process, but it is fixed by the $K^+\Sigma^0$ and $K^0\Sigma^+$ photoproduction channels, for which more experimental data with better statistics are available. Changing the value of $r_{K_1K\gamma}$ will obviously change the predicted observables in the $K^0\Sigma^+$ channel. Furthermore, we also note that the elementary amplitude used to extract the cross section (called SLA in [2]) fits relatively older data. In the previous work [8] we used more recent data and found that the new electroproduction data provide a stringent constraint to the background, especially to the K_1 contribution.

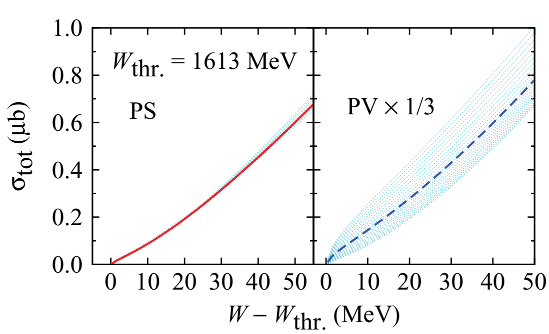

FIG. 2. (Color online) Total cross sections of the $\gamma + n \to K^0 + \Lambda$ channel predicted by the models using PS (left panel) and PV (right panel) couplings. The shaded area corresponds to the variation of the the ratio $r_{K_1K\gamma}$ in Eq. (3). The PV cross section has been renormalized by a factor of 1/3.

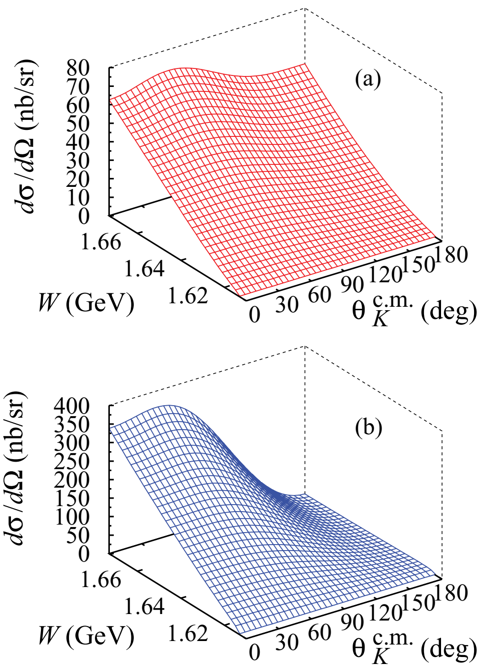

FIG. 3. (Color online) Differential cross sections of the $\gamma + n \to K^0 + \Lambda$ channel predicted by the models using pseudoscalar (a) and pseudovector (b) couplings.

The extension of the PS model to the case of electroproduction has been also discussed in our previous report [8]. Fortunately, experimental data are also available for the $K^+\Lambda$ electroproduction near threshold so that all unknown longitudinal/scalar couplings can be directly extracted. However, this is not the case in the $K^0\Lambda$ electroproduction. Thus, the required scalar photon coupling of the $S_{11}(1650)$ resonance amplitude is taken from the MAID2007 model [4,10], i.e., $S^n_{1/2} = 0.010\ \ \mathrm{GeV}^{-1/2}$. The neutron electromagnetic form factors are taken from the Galster parameterization [11], whereas the hyperon form factors as well as the dependencies of the electric and scalar multipoles on Q^2 are assumed to have the same forms as in the $K^+\Lambda$ channel [8].

Compared with other neutral SU(3) pseudoscalar mesons, the neutral kaon has a unique property, i.e., it has an electric or charge form factor. The difference between the strange and ordinary quark masses creates a nonuniform charge distribution in the K^0. Consequently, although its total charge is zero, the K^0 has an electric or charge form factor. Since the mass difference is still smaller than the mass scale associated with confinement in quantum chromodynamics

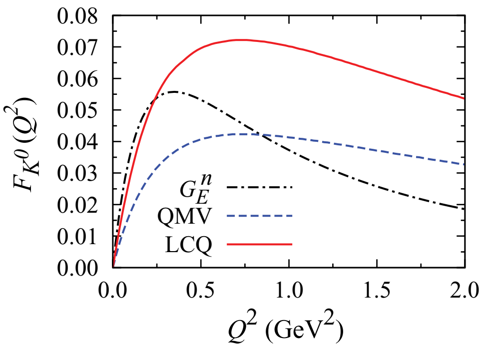

FIG. 4. (Color online) Electromagnetic form factors of the neutral kaon predicted by the quark meson vertex (QMV) and light cone quark (LCQ) models compared with the electric form factor of the neutron G_E^n.

(QCD), $(m_s - m_d) < \Lambda_{\rm QCD}$, it could lead to a sensitive test of phenomenological models that attempt to describe nonperturbative QCD.

In this paper we do not intend to discuss the form factor in detail; instead we only employ two relativistic quark models, the light-cone quark (LCQ) model [12] and the quark-meson vertex (QMV) model [13], in order to find the optimal kinematics where this form factor has the largest effect on the observable. Since contributions of the K^* and K_1 exchanges are relatively small in the PS model, contribution of the kaon pole is expected to generate sizable effects on the cross section. The characteristic of these two form factors is exhibited in Fig. 4, where the charge form factor of the neutron $G_E^n(Q^2)$ [11] is also shown for comparison. It is clear from this figure that they have comparable magnitudes. The only difference is that as Q^2 increases the two neutral kaon form factors fall off slower than the neutron one.

We note that the inclusion of the K^0 form factor is connected with the problem of gauge invariance. In this work we have utilized the Fubini-Nambu-Wataghin term [14] to restore gauge invariance, which is discussed in Ref. [15]. Since the term is very specific and not trivial, we expect that different methods of restoring gauge invariance in this process will not affect the result shown in this work.

The effect of the QMV and LCQ form factors on the separated differential cross sections of the $K^0\Lambda$ electroproduction on a neutron is displayed in Fig. 5, where we have chosen a closer kinematics as in the case of the $K^+\Lambda$ [8], since we expect that with the present technology such a kinematics is experimentally accessible. From this figure it is apparent that the observed effect in the cross-section magnitude is consistent with the behavior of the form factors exhibited in Fig. 4, i.e., the LCQ model yields the strongest effect.

The effect of K^0 form factors on the unpolarized cross section σ_U shown in the upper panels of Fig. 5 seems to be mild, in contrast to the effect on the separated cross sections σ_{TT} and σ_{LT}. This is true especially in the case of the interference cross section σ_{LT} shown in the bottom panels of Fig. 5, where the effect of the LCQ model is predicted to be around 30% at $Q^2 = 0.65$ GeV^2. However, we found that the effect is almost negligible on the transversely unpolarized cross section

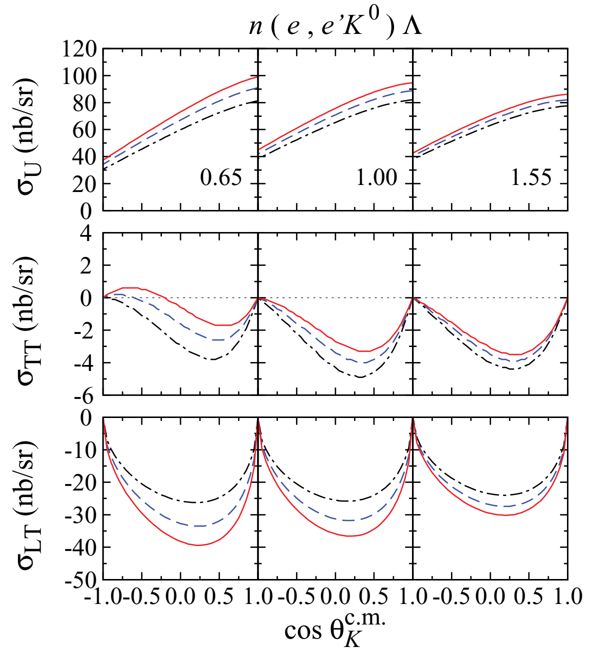

FIG. 5. (Color online) Separated differential cross sections for the neutral kaon electroproduction $e + n \to e' + K^0 + \Lambda$ as a function of the kaon scattering angle at $W = 1.65$ GeV and for different values of Q^2 (shown in the top panels in units of GeV^2). Solid lines show the calculation with a K^0 form factor obtained in the LCQ model while dashed lines are obtained by using the QMV model. The dash-dotted lines are obtained from a computation with the K^0 pole excluded. Note that $\sigma_U = d\sigma_T/d\Omega_K + \epsilon d\sigma_L/d\Omega_K$, $\sigma_{TT} = d\sigma_{TT}/d\Omega_K$, and $\sigma_{LT} = d\sigma_{LT}/d\Omega_K$.

$d\sigma_T/d\Omega$. Therefore, the difference between the three lines shown in this figure originates mostly from the longitudinal cross section $d\sigma_L/d\Omega$. Consequently, we focus our analysis on the longitudinal cross section. The effects for different values of kaon scattering angle are shown in Fig. 6. It is obvious that the effect is sufficiently large for an experimental check and in fact, at the forward angle $\theta_K^{\rm c.m.} = 25.84^\circ$ and $Q^2 \approx 0.5$ GeV^2, the LCQ form factor raises the cross section to 50%. As explained above, this phenomenon originates from the dominant role of the background terms. From this figure it is also clear that as the scattering angle increases the effect slightly decreases, but it is still relatively large for the LCQ model at $\theta_K^{\rm c.m.} = 126.87^\circ$. Our finding therefore corroborates the finding of Ref. [7], which used the same form factors [12,13] as in the present work but with a different isobar model [16]. Experimental data with about 10% uncertainty would be able to resolve the effect of the form factors or even to pin down the appropriate K^0 form factor required by the isobar model to describe the $e + n \to e' + K^0 + \Lambda$ process.

In conclusion, we have extended our previous isobar model for the $K^+\Lambda$ channel to include both photo- and electroproduction of $K^0\Lambda$ by exploiting the SU(3) symmetry and appropriate information from the *Particle Data Book*. Using this model we have also analyzed the differences in the total and differential cross sections obtained by using PS and

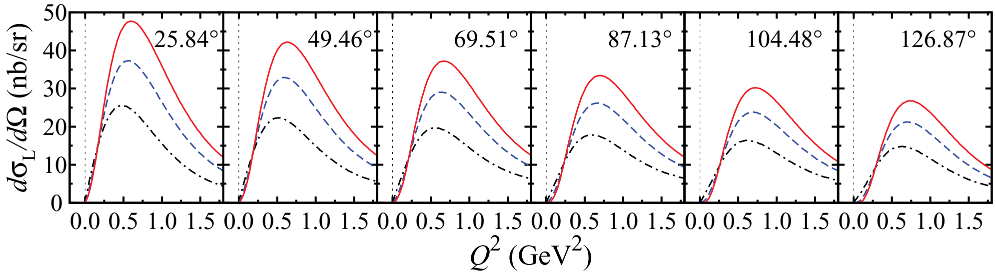

FIG. 6. (Color online) Longitudinal differential cross section of the neutral kaon electroproduction $e + n \rightarrow e' + K^0 + \Lambda$ as a function of the virtual photon momentum squared Q^2 at $W = 1.65$ GeV and for different values of the kaon scattering angles (shown inside the panels). Notation of the curves is as in Fig. 5.

PV couplings. It is found that the PV model yields significantly larger total and differential cross sections. Needless to say, experimental data on the $K^0\Lambda$ photoproduction are required to check this phenomenon. We have also used the PS model to explore the effect of the K^0 charge form factor and found sizable effects on the longitudinal and interference cross sections of the $K^0\Lambda$ electroproduction. Especially in the longitudinal cross section, we found that the effect could raise the cross section up to 50%.

The author acknowledges support from the University of Indonesia and a Competence Grant from the Indonesian Ministry of National Education.

[1] A. Salam, K. Miyagawa, T. Mart, C. Bennhold, and W. Glöckle, Phys. Rev. C **74**, 044004 (2006).
[2] K. Tsukada *et al.*, Phys. Rev. C **78**, 014001 (2008).
[3] T. Mart and C. Bennhold, Phys. Rev. C **61**, 012201 (1999).
[4] T. Mart and A. Sulaksono, Phys. Rev. C **74**, 055203 (2006).
[5] T. Mart, C. Bennhold, and C. E. Hyde Wright, Phys. Rev. C **51**, 1074 (1995).
[6] Available at the Maid homepage [http://www.kph.uni-mainz.de/MAID/kaon/kaonmaid.html]. The published versions can be found in Ref. [3]; T. Mart, Phys. Rev. C **62**, 038201 (2000); C. Bennhold, H. Haberzettl, and T. Mart, in *Proceedings of 2nd ICTP International Conference on Perspectives in Hadronic Physics*, edited by S. Boffi *et al.*, Trieste, Italy, 1999, p. 328.
[7] T. Mart and C. Bennhold, Nucl. Phys. A **639**, 237 (1998).
[8] T. Mart, Phys. Rev. C **82**, 025209 (2010).
[9] K. Nakamura *et al.*, J. Phys. G **37**, 075021 (2010).
[10] D. Drechsel, S. S. Kamalov, and L. Tiator, Eur. Phys. J. A **34**, 69 (2007).
[11] S. Galster, H. Klein, J. Moritz, K. H. Schmidt, D. Wegener, and J. Bleckwenn, Nucl. Phys. B **32**, 221 (1971).
[12] C. Bennhold, H. Ito, and T. Mart, *Proceedings of the 7th International Conference on the Structure of Baryons*, Santa Fe, NM, 1995, p. 323.
[13] W. W. Buck, R. Williams, and H. Ito, Phys. Lett. B **351**, 24 (1995); H. Ito and F. Gross, Phys. Rev. Lett. **71**, 2555 (1993).
[14] S. Fubini, Y. Nambu, and V. Wataghin, Phys. Rev. **111**, 329 (1958).
[15] B. B. Deo and A. K. Bisoi, Phys. Rev. D **9**, 288 (1974).
[16] R. A. Williams, C.-R. Ji, and S. R. Cotanch, Phys. Rev. C **46**, 1617 (1992).